THE JOURNAL OF PHYSICAL CHEMISTRY Letters

Letter

Cite This: J. Phys. Chem. Lett. 2019, 10, 4968−4973

pubs.acs.org/JPCL

Nanoparticle Loading of Unentangled Polymers Induces Entanglement-Like Relaxation Modes and a Broad Sol−Gel Transition

Xue-Zheng Cao,*[,¶,⊥,#] Holger Merlitz,[‡] and M. Gregory Forest*[,¶]

[‡]Leibniz-Institut für Polymerforschung Dresden, 01069 Dresden, Germany

[¶]Departments of Mathematics and Applied Physical Sciences, University of North Carolina at Chapel Hill, Chapel Hill, North Carolina 27599-3250, United States

[⊥]Department of Physics, Xiamen University, Xiamen 361005, P.R. China

Supporting Information

ABSTRACT: We combine molecular dynamics simulations, imaging and data analysis, and the Green−Kubo summation formula for the relaxation modulus $G(t)$ to elicit the structure and rheology of unentangled polymer−nanoparticle composites distinguished by small NPs and strong NP−monomer attraction, $\varepsilon_{NPM} \gg k_BT$. A reptation-like plateau emerges in $G(t)$ beyond a terminal relaxation time scale as the volume fraction, c_{NP}, of NPs increases, coincident with a structure transition. A condensed phase of NP-aggregates forms, tightly interlaced with thin sheets of polymer chains, the remaining phase consisting of free chains void of NPs. Rouse mode analyses are applied to the two individual phases, revealing that long-wavelength Rouse modes in the aggregate phase are the source of reptation-like relaxation. Imaging reveals chain motion confined within the thin sheets between NPs and exhibits a 2D analogue of classical reptation. In the NP-free phase, Rouse modes relax indistinguishable from a neat polymer melt. The Fourier transform of $G(t)$ reveals a sol−gel transition across a broad frequency spectrum, tuned by c_{NP} and ε_{NPM} above critical thresholds, below which all structure and rheological transitions vanish.

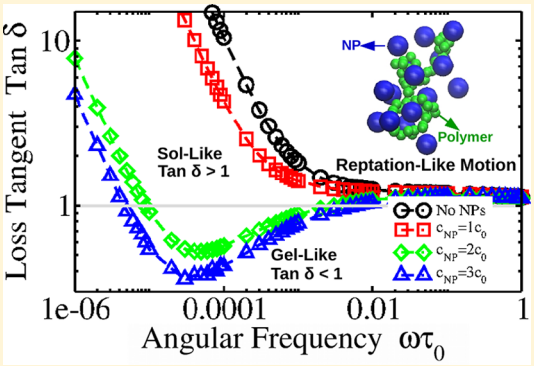

The loading of nanoparticles (NPs) into polymeric matrices generally yields a mechanical reinforcement of the polymer nanocomposites (PNCs) relative to the neat polymer host, even at low NP loadings.[1−3] The growing availability of NPs with controllable affinities and the development of instrumentation to probe small length scales have spurred renewed studies in mechanical reinforcement as well as viscoelasticity of PNCs.[4−9] A detailed study of the mutual interplay between NPs and host polymer chains, linking structural properties, modified relaxation dynamics of polymer chains and NPs, and dynamic mechanical and rheological properties of PNCs, is imperative for quantitative and predictive engineering of function-specific PNCs.[10−15]

The distribution of NPs in polymers depends strongly on the enthalpic interaction between NPs and polymers. When there is no favorable polymer−NP attraction, an athermal system with its morphology being determined by conformational entropic effects,[16] the polymer is depleted at NP surfaces, leading to bare NP aggregation and reduced surface contacts between NPs and monomers.[17−19] Such situations degrade the intended boosts in mechanical and rheological PNC properties. As a result of counteracting the entropy-favored direct surface contact of NPs, a favorable NP−polymer attraction or grafting of polymers onto NPs is pursued to achieve good dispersions of NPs.[20,21] As the polymer−NP attraction gets stronger, a re-entrant aggregation structure of polymer-bound NPs emerges in PNCs in which there is a polymer layer surrounding the surface of individual NPs, which then induces an effective attraction between the polymer-dressed NPs.[22−24] In the presence of strong NP−polymer attraction, the morphology of polymer chains and the distribution of NPs are dominated by the enthalpic NP−polymer attraction. Dynamic neutron scattering and dielectric experiments show that the polymer chains at the surface of NPs are still mobile with no glassy nature, while their center-of-mass diffusion and certain Rouse relaxation modes are suppressed due to adsorption.[25−27] In a recent study using X-ray photon correlation spectroscopy to observe the motion of silica NPs diffusing in an attractive poly(ethylene oxide) melt, Senses et al. found that the NPs unexpectedly remain mobile at a high volume fraction (c_{NP}) of NPs, even though the elastic modulus of the silica−PEO composites increases by 3 orders of

Received: July 6, 2019
Accepted: August 6, 2019
Published: August 6, 2019

DOI: 10.1021/acs.jpclett.9b01954
J. Phys. Chem. Lett. 2019, 10, 4968−4973

magnitude.[28] These results confirm the mobilities of polymer chains and NPs even though they are strongly constrained at high loadings of NPs and in the presence of strong polymer−NP attraction. The present study provides physical explanation and mechanistic understanding of how highly attractive, NP−polymer interactions in an unentangled polymer host can induce tunable mechanical reinforcement and a sol−gel transition over broad frequencies.

Molecular dynamics (MD) simulations of bead−spring polymer chains were performed for PNCs over a two-parameter range of attraction strengths ε_{NPM} and NP concentrations c_{NP}. Experiments have shown that a reduction in NP size, with attractive NP−polymer interactions, results in increased mechanical reinforcement.[5] Therefore, a lower c_{NP} is sufficient with smaller NPs to achieve a desired increase in the elastic modulus of PNCs. In light of this result, we are led to explore PNCs where the monomer size (bead diameter), σ_M, and NP diameter, σ_{NP}, are of comparable size, $\sigma_{NP} = 3\sigma_M$. In the model, interchain chemical bonds are enforced by a finitely extensible nonlinear elastic (FENE) potential.[29] Monomer−monomer and NP−NP interactions are modeled as approximate hard-sphere potentials to avoid enthalpic energy gain when they come into close proximity. There is an excess enthalpic energy gain ε_{NPM} for monomer−NP contact interactions. The equation of motion for the displacement of a particle (monomer or NP) is given by the Langevin equation.[30,31] The volume fractions of monomers $c_M = N_M \frac{4}{3}\pi\left(\frac{\sigma_M}{2}\right)^3 \frac{1}{V}$ and NPs $c_{NP} = N_{NP}\frac{4}{3}\pi\left(\frac{\sigma_{NP}}{2}\right)^3 \frac{1}{V}$ are adopted to quantify the bulk concentrations of polymers and NPs, where V, N_M, and N_{NP} are the system volume and total number of monomers and NPs, respectively. Simulations were carried out using the open-source LAMMPS MD package. Further modeling details are available in the Supporting Information.

Simulations were first performed to generate sufficient data to compute the stress relaxation modulus, $G(t)$, of PNCs versus c_{NP}.[32−34] As revealed in Figure 1a, free chains in the neat polymer melt are unentangled, with the corresponding $G(t)$ being well described by the stress relaxation modulus function for unentangled polymers[35]

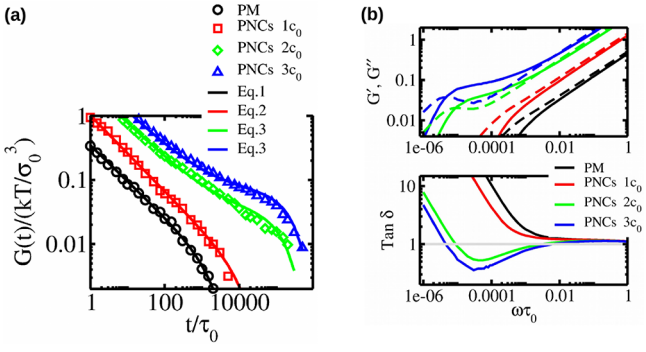

Figure 1. Linear rheology of the baseline neat polymer melt and PNCs at different NP volume fractions. (a) Stress relaxation modulus, with simulation data shown in open symbols and the corresponding fits shown in solid curves. (b) Storage (solid) and loss (dashed) moduli and loss tangent (lower panel). The polymer chain length is $N = 64$, the NP−monomer attraction strength is $\varepsilon_{NPM} = 8.0k_BT$, the monomer volume fraction is $c_M = 36\%$, and the baseline NP volume fraction is $c_0 = 2.6\%$.

$$G_{PM}(t) = n_m \cdot k_B T \cdot \left(\frac{t}{\tau_m}\right)^{\gamma} \cdot \exp\left(-\frac{t}{\tau_{ter}}\right) \quad (1)$$

in which $n_m = \frac{N_M}{V} = 0.68$ gives the number density of monomers, and the fitting parameters are estimated numerically, with $\gamma \approx -0.56$, the monomeric relaxation time $\tau_m = 0.30\tau_0$, and the terminal relaxation time of polymer chains $\tau_{ter} = 2.2 \times 10^3\tau_0$, with τ_0 being the time scale unit. Upon adding NPs, $G(t)$ for the baseline NP volume fraction $c_{NP} = c_0 = 2.6\%$ is well-fitted by a rescaled form of eq 1

$$G_{PNC}(t) = G_{PM}(t/a_{shift}) = n_m \cdot k_B T \cdot \left(\frac{t}{a_{shift} \cdot \tau_m}\right)^{\gamma} \cdot \exp\left(-\frac{t}{a_{shift} \cdot \tau_{ter}}\right) \quad (2)$$

in which $a_{shift} \approx 6.5$ gives the horizontal rescaling factor of $G_{PNC}(t)$ relative to $G_{PM}(t)$. The rescaled $G(t)$ indicates that at low $c_0 = 2.6\%$ the effect of NPs is to damp or retard the polymer relaxation dynamics almost identically on all length scales from one monomer to the entire polymer chain.

Maintaining strong NP−monomer attraction energy, a plateau in $G(t)$ begins to emerge when the NP volume fraction is doubled, $c_{NP} = 2c_0$, and further strengthens at three times the unit NP loading, Figure 1a. A plateau in $G(t)$ is the classic signature of reptation of entangled polymer melts. A modified scaling formula including a smooth crossover between the Rouse and reptation relaxation regimes was adopted to fit the direct simulation data of the stress relaxation modulus of the corresponding PNCs

$$G_{PNCs}(t) = n_m \cdot k_B T \cdot \left[\left(\frac{t}{a_{shift}^{Mon} \cdot \tau_m}\right)^{\gamma} + G_e\right] \cdot \exp\left(-\frac{t}{a_{shift}^{Ter} \cdot \tau_{ter}}\right) \quad (3)$$

where these scaling parameters for $c_{NP} = 2c_0$ and $3c_0$ are given by plateau modulus $G_e = 4.1 \times 10^{-2}$ and 9.1×10^{-2}, the monomeric shift factor $a_{shift}^{Mon} = 40$ and 82, and the terminal shift factor $a_{shift}^{Ter} = 66$ and 1.1×10^2, respectively. These results indicate that the macroscopic linear rheology of PNCs for $c_{NP} = 2c_0$ and $3c_0$ resembles that of an entangled neat polymer melt with entanglement length $N_{ent} = \frac{k_B T}{G_e}$ and the monomeric and terminal relaxation time $a_{shift}^{Mon}\tau_M$ and $a_{shift}^{Ter}\tau_{ter}$, respectively. The modified relaxation spectrum of polymer chains and the resulting sol−gel transition are induced above sufficiently high NP loadings and sufficiently strong NP−monomer attraction strength. The complex modulus, $G^*(\omega)$, is the Fourier transform of $G(t)$, with the storage (elastic) moduli $G'(\omega)$ and loss (viscous) moduli $G''(\omega)$ given by the real and imaginary parts: $G^*(\omega) = G'(\omega) + iG''(\omega)$, where $\omega = 2\pi/t$ is the angular frequency. Figure 1b gives the results of $G'(\omega) = \omega \int_0^\infty G(t)\cdot\sin(\omega t)\, dt$, $G''(\omega) = \omega \int_0^\infty G(t)\cdot\cos(\omega t)\, dt$, and the loss tangent, $\tan\delta(\omega) = \frac{G''(\omega)}{G'(\omega)}$. A viscoelastic material is *gel-like* at frequency ω if $\tan\delta(\omega) < 1$ and *sol-like* if $\tan\delta(\omega) > 1$. Figure 1b clearly reveals a sol−gel transition over a broad intermediate-frequency range when the volume fraction of NPs is $c_{NP} = 2c_0$ and $3c_0$.

In the presence of a strong NP−monomer attraction with $\varepsilon_{NPM} \gg k_BT$, a stable adsorption layer of polymer chains self-assembles from an initial homogeneous NP dispersion, with single chains intertwining tightly packed, small NPs; cascading

DOI: 10.1021/acs.jpclett.9b01954
J. Phys. Chem. Lett. 2019, 10, 4968−4973

out in scale, one finds phase-separated aggregates of NPs woven together by thin, wavy sheets of polymer chains, segregated from NP-void domains of free chains.[22−24] This phase separation structure is shown in Figure 2: (1) inside

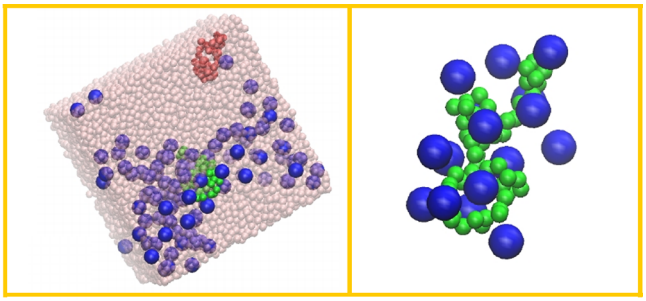

Figure 2. Structure snapshot of a PNC system (with $c_{NP} = 2c_0$ and $\varepsilon_{NPM} = 8k_BT$) at equilibrium: NP-rich and NP-void phase separation. NPs (blue), monomers of a single polymer chain inside of the NP-rich phase (green), and monomers of a single polymer chain inside of the NP-void phase (red) are shown. All other polymer chains (gray) are transparent in the right snapshot and not shown in the right column.

polymer refers to polymer chains inside of the NP-rich aggregate phase, and (2) outside polymer refers to polymer chains without contact with NPs. For inside polymer chains, there are combined effects arising from the strong polymer−NP attraction and jamming within NP aggregates,[36,37] both suppressing the mobility of polymer segments. Simultaneously, the relaxation dynamics of outside polymer chains are minimally affected because NP−polymer attraction and jamming are both absent. As a result, we anticipate a significant difference in the relaxation dynamics between the inside polymer and outside polymer chains, as experimentally reported by Senses et al.[38]

To quantify this intuition, a Rouse mode analysis is now presented separately for the relaxation spectra of inside polymer NP−aggregate chains and outside polymer NP-free chains and thereby show their relative contributions to the full PNC relaxation spectrum, reptation-like plateau, and sol−gel transition at sufficiently high NP loading and NP−monomer attraction strength $\varepsilon_{NPM} \gg k_BT$. It was theoretically predicted and verified in simulations that the averaged autocorrelation function of the pth Rouse mode, representing the relaxation dynamics of a polymer subchain including $\frac{N-1}{p}$ beads, can be well described by a stretched exponential: $\boldsymbol{X}_p(t) \cdot \boldsymbol{X}_p(0) = \langle \boldsymbol{X}_p{}^2 \rangle \exp\left[-\left(\frac{t}{\tau_p}\right)^{\beta_p}\right]$,[39,40] in which τ_p and β_p are the relaxation times of the pth mode and the corresponding stretching factor, respectively. β_p characterizes the distribution of relaxation times of the pth mode, which indicates a simple exponential decay if $\beta_p = 1$ or a decay with broader relaxation distributions if $\beta_p < 1$. The effective monomeric relaxation rate was computed as $W^{eff} = \frac{1}{4\tau_p^{eff} \sin^2\left(\frac{p\pi}{2N}\right)}$, where the effective relaxation time of the pth mode $\tau_p^{eff} = \int_0^\infty \exp\left[-\left(\frac{t}{\tau_p}\right)^{\beta_p}\right] dt$. Note that neither W^{eff} nor β_p have any dependence on the mode number for ideal Rouse chains. The simulation results of $\langle \boldsymbol{X}_p(t) \cdot \boldsymbol{X}_p(0) \rangle$, W^{eff}, and β_p for the inside polymer and outside polymer chains are given in Figure 3. The values of both W^{eff}

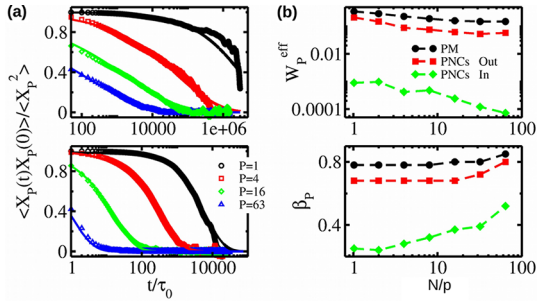

Figure 3. Rouse mode analysis of the relaxation of polymer chains. (a) Upper and lower panels give the autocorrelation functions of the Rouse modes of polymer chains inside and outside of the NP-rich aggregate phase, respectively. (b) Effective monomeric relaxation rates (upper panel) and stretching parameters (lower panel) for pure polymer melt chains (shown in black) and polymer chains inside (green) and outside (red) of the NP-rich aggregate phase. Here, $c_{NP} = 2c_0$ and $\varepsilon_{NPM} = 8k_BT$.

and β_p for outside polymer chains are the counterparts for chains in the neat polymer melt. The decline is almost the same for both the monomeric relaxation rate and the stretching factor versus mode number p, corresponding to length scale $\frac{N-1}{p}$. The unchanged relaxation spectrum of outside polymer chains indicates that outside polymer chains behave like a renormalized polymer melt in which the rescaling factor $a_{shift}^{Out} = W_{PM}^{eff}(p)/W_{Out}^{eff}(p)$ is p-invariant. Therefore, we find $G_{Out}(t) = G_{PM}(t/a_{shift}^{Out})$ for the stress relaxation modulus of outside polymer chains.

The relaxation of inside polymer chains is considerably slower for all modes, i.e., on all length scales, compared to the relaxation of outside polymer chains. With increasing $\frac{N}{p}$, W^{eff} for inside polymer chains decreases, accompanied by an increase of β_p. Moreover, the corresponding rescaling factor of $a_{shift}^{In}(p) = W_{PM}^{eff}(p)/W_{In}^{eff}(p)$ decreases versus p. Note that the value of a_{shift}^{In} should be constant independent of p if the NP constraints that retard the motion of unentangled Inside polymer chains are length scale-invariant. Signatures shown in W^{eff} and β_p indicate that the inside polymer chains are exposed to stronger constraints by the NPs, leading to narrowed relaxation distributions on longer length scales, i.e., at larger $\frac{N-1}{p}$. On the other hand, the adsorption thickness of inside polymer chains bound on the surface of NPs, for $\varepsilon_{NPM} \gg k_BT$, is of the same order as the bead size.[24,41] Therefore, the inside polymer chains are constrained to motion within the thin adsorption sheets between NPs in the NP-aggregate phase, with strongly suppressed motion normal to NP surfaces. Each inside polymer chain that adsorbs simultaneously on several different NPs is restricted to motion along and within these thin, 2D, wavy sheets, relaxing due to the adsorption confinement of NPs. Figure 1 in the Supporting Information shows a sequence of snapshots of the reptation-like configurational mobility of a single inside polymer chain with a very weak pulling force applied to one end.

We propose that the constraints "felt" by inside polymer chains on larger length scales arise from a 2D analogue of reptation within the thin, wavy sheets that intertwine the NP aggregates. Therefore, the stress relaxation modulus of inside polymer chains has the following expression

DOI: 10.1021/acs.jpclett.9b01954
J. Phys. Chem. Lett. 2019, 10, 4968−4973

$$G_{\mathrm{In}}(t) = n_{\mathrm{m}} \cdot k_{\mathrm{B}}T \cdot \left[\left(\frac{t}{a_{\mathrm{shift}}^{\mathrm{InMon}} \tau_{\mathrm{m}}} \right)^{\gamma} + \frac{1}{N_{\mathrm{ent}}^{\mathrm{eff}}} \right] \cdot \exp\left(-\frac{t}{a_{\mathrm{shift}}^{\mathrm{InTer}} \tau_{\mathrm{ter}}} \right) \quad (4)$$

with $a_{\mathrm{shift}}^{\mathrm{InMon}} = W_{\mathrm{PM}}^{\mathrm{eff}}(p = N-1)/W_{\mathrm{In}}^{\mathrm{eff}}(p = N-1)$; $a_{\mathrm{shift}}^{\mathrm{InTer}}$ is the shift fator of the terminal relaxation time, and $N_{\mathrm{ent}}^{\mathrm{eff}}$ is "an effective tube diameter" that gives the same free volume as the confinement sheet. The stress relaxation modulus of the full PNC system is well fit by the sum of contributions from inside polymer and outside polymer chains

$$G_{\mathrm{PNCs}}(t) = \phi_{\mathrm{Out}} \cdot G_{\mathrm{Out}}(t) + \phi_{\mathrm{In}} \cdot G_{\mathrm{In}}(t) \quad (5)$$

with ϕ_{Out} and $\phi_{\mathrm{In}} = 1 - \phi_{\mathrm{Out}}$ being the percentages of outside polymer and inside polymer chains, respectively. As shown in Figure 4, the theoretical prediction of eq 5 derived from the primary effect is a concentration-dependent relaxation delay. The relaxation dynamics of polymer chains on all length scales, from one monomer to the whole chain, are uniformly slowed down by the presence of NPs, quite the same as a reduced temperature effect for neat polymer melts. A Williams−Landel−Ferry (WLF) model is generally used to quantify the time−temperature superposition of dynamic relaxation of polymer systems. We confirmed in the simulations, as shown in the inset of Figure 5, that the rescaling factor of $G_{\mathrm{PNCs}}(t)$ for weakly attractive PNCs relative to $G_{\mathrm{PM}}(t)$ for the neat polymer melt can be well-fit by a WLF-like formula used to describe the time−NP concentration superposition

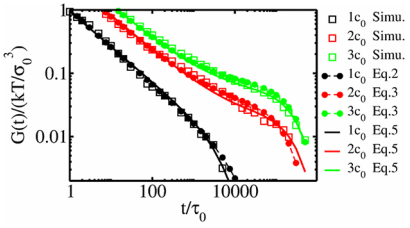

Figure 4. Theoretical fitting of eq 5 to the simulation data of the stress relaxation modulus of PNCs, for the cases shown in Figure 1. Note that $N_{\mathrm{ent}}^{\mathrm{eff}}$ and $a_{\mathrm{shift}}^{\mathrm{InTer}}$ are the free fitting parameters. Here, ϕ_{Out} = 99, 77, and 69% for the cases of $c_{\mathrm{NP}} = c_0$, $2c_0$, and $3c_0$, respectively. The method for computing ϕ_{Out} is provided in the Supporting Information.

Rouse mode analysis fits well to the direct simulation data of $G_{\mathrm{PNCs}}(t)$. The effective diameter of the confinement tube is $N_{\mathrm{ent}}^{\mathrm{eff}}$ = 63, 7.7, and 4.2 for the cases of $c_{\mathrm{NP}} = c_0$, $2c_0$, and $3c_0$, respectively. $N_{\mathrm{ent}}^{\mathrm{eff}} \approx N$ for the case of $c_{\mathrm{NP}} = c_0$ indicates that the confinement constraint of NPs on inside polymer chains is very weak, and a plateau is therefore absent in $G_{\mathrm{PNCs}}(t)$.

Finally, we compare and contrast the above results for strong NP−polymer attraction with weak attraction, $\varepsilon_{\mathrm{NPM}} \approx O(k_{\mathrm{B}}T)$. The aggregation of polymer-coated NPs disappears due to the weakened "effective bridging attraction".[42] The homogeneous dispersion of NPs is thereby maintained. Equivalently, the enthalpic energy gain due to NP−polymer attraction is insufficient to counteract the entropy loss of adsorbing polymer chains,[24,41] and therefore, the bridging interaction between polymer-coated NPs is not entropically favored. In addition, for the NP and monomer size scales considered here, $\sigma_{\mathrm{NP}} = 3\sigma_{\mathrm{M}}$, and $\varepsilon_{\mathrm{NPM}} = k_{\mathrm{B}}T$, the adsorption lifetime of polymer chains around each NP is shorter than the crossover time of the NP from subdiffusive to normal diffusive scaling.[41] Therefore, the constrained relaxation of adsorbing polymer chains on NPs is minimal, preventing stable jamming of NPs and favoring a homogeneous dispersion. In this scenario, one anticipates a simple rescaling of the PNC relaxation modulus to the neat polymer melt. Indeed, as shown in Figure 5, the stress relaxation moduli for $\varepsilon_{\mathrm{NPM}} = k_{\mathrm{B}}T$ versus increasing volume fraction of NPs can be rescaled to match $G(t)$ of the neat polymer melt, using eq 2. These results indicate that there is no dramatic volume-fraction-dependent rheological effect on PNCs with weak NP−polymer attraction. The relaxation spectrum of polymer chains in PNCs is therefore not modified with increasing volume fraction when $\varepsilon_{\mathrm{NPM}} = k_{\mathrm{B}}T$; instead, the

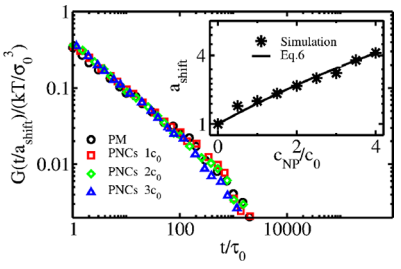

Figure 5. Rescaled stress relaxation moduli of PNCs when the attraction strength is weak, $\varepsilon_{\mathrm{NPM}} = k_{\mathrm{B}}T$, versus the NP volume fraction c_{NPM}, using eq 2 as the rescaling function and the neat polymer melt system as the baseline for reference. The inset gives the shift factor as a function of the NP volume fraction.

$$a_{\mathrm{shift}}(c_{\mathrm{NP}}) = \exp\left(\frac{A_1 c_{\mathrm{NP}}}{A_2 + c_{\mathrm{NP}}} \right) \quad (6)$$

where A_1 = 7.8 (unitless) and A_2 = 18 (in units of c_0) for $\varepsilon_{\mathrm{NPM}} = 1k_{\mathrm{B}}T$.

In summary, we employ MD simulations of unentangled polymer−NP composites, focusing on small NPs at sufficiently high NP loading and with sufficiently strong NP−monomer attraction. The simulated data, Rouse mode analyses, and imaging reveal a structure transition marked by a NP-rich aggregate phase and a NP-void phase, with very thin sheets of polymer chains interweaving the dense NP aggregates; a reptation-like plateau in the stress relaxation modulus, dominated by the chains confined within the 2D sheets within NP-rich aggregates; and a sol−gel rheological transition at sufficiently high loading and NP−monomer attraction energy, across a spectrum tunable by both loading and attraction strength. Furthermore, the NP-free chains relax indistinguishable from chains in the neat polymer melt. All features of these PNCs (structure transition into dense NP aggregates and NP-free domains, a reptation-like plateau in the relaxation modulus, and a broad frequency sol−gel transition) vanish as the NP−polymer attraction strength is reduced to $\varepsilon_{\mathrm{NPM}} = k_{\mathrm{B}}T$ or as the NP loading drops. In the weak NP−monomer attraction regime, the presence of NPs uniformly delays the relaxation of polymer chains, consistent with a reduction of the temperature in a neat polymer melt. Of primary interest for practical applications of PNCs is the ability to control dynamical mechanical properties. Both the NP volume fraction and NP−polymer attraction strength are quantities that are easily tuned in the laboratory. As recently observed, NPs can facilitate disentanglement in entangled polymer−NP composites, thus affecting their rheological properties due to the dilution of entanglements.[38,43] The entanglement concen-

DOI: 10.1021/acs.jpclett.9b01954
J. Phys. Chem. Lett. 2019, 10, 4968−4973

tration regime in the presence of a strong NP−monomer attraction will be discussed in a future submission.

■ ASSOCIATED CONTENT

Supporting Information

The Supporting Information is available free of charge on the ACS Publications website at DOI: 10.1021/acs.jpclett.9b01954.

Details of the molecular dynamics model; computation of the stress relaxation modulus; categories of inside polymer and outside polymer chains; computation of Rouse modes; and snapshots showing structure change of a single inside polymer chain diffusing within the NP aggregate (PDF)

■ AUTHOR INFORMATION

Corresponding Authors

*E-mail: xzcao@xmu.edu.cn.
*E-mail: forest@unc.edu.

ORCID

Xue-Zheng Cao: 0000-0002-0409-6324

Present Address

#Department of Physics, Xiamen University, Xiamen 361005, P.R. China.

Notes

The authors declare no competing financial interest.

■ ACKNOWLEDGMENTS

This research was supported in part by the National Science Foundation through Grants DMS-1462992, DMS-1517274, and DMS-1664645. The authors acknowledge valuable conversations with colleagues Ronit Freeman, Boyce Griffith, and David Hill.

■ REFERENCES

(1) Balazs, A. C.; Emrick, T.; Russell, T. P. Nanoparticle Polymer Composites: Where Two Small Worlds Meet. *Science* **2006**, *314*, 1107−1110.

(2) Hussain, F.; Hojjati, M.; Okamoto, M.; Gorga, R. E. Polymer-Matrix Nanocomposites, Processing, Manufacturing, and Application: An Overview. *J. Compos. Mater.* **2006**, *40*, 1511−1575.

(3) Crosby, A. J.; Lee, J. Y. Polymer Nanocomposites: The "Nano" Effect on Mechanical Properties. *Polym. Rev.* **2007**, *47*, 217−229.

(4) Choi, H. J.; Ray, S. S. A Review on Melt-State Viscoelastic Properties of Polymer Nanocomposites. *J. Nanosci. Nanotechnol.* **2011**, *11*, 8421−8449.

(5) Appel, E. A.; et al. Self-Assembled Hydrogels Utilizing Polymer-Nanoparticle Interactions. *Nat. Commun.* **2015**, *6*, 6295.

(6) Boland, C. S.; et al. Sensitive Electromechanical Sensors Using Viscoelastic Graphene-Polymer Nanocomposites. *Science* **2016**, *354*, 1257−1260.

(7) Hiremath, V.; Shukla, D. K. Effect of Particle Morphology on Viscoelastic and Flexural Properties of Epoxy-Alumina polymer Nanocomposites. *Plast., Rubber Compos.* **2016**, *45*, 199−206.

(8) Newby, J.; Schiller, J. L.; Wessler, T.; Edelstein, J.; Forest, M. G.; Lai, S. A Blueprint for Robust Crosslinking of Mobile Species in Biogels with Weakly Adhesive Molecular Anchors. *Nat. Commun.* **2017**, *8*, 833.

(9) Newby, J. M.; Schaefer, A. M.; Lee, P. T.; Forest, M. G.; Lai, S. K. Convolutional Neural Networks Automate Detection for Tracking of Submicron-Scale Particles in 2D and 3D. *Proc. Natl. Acad. Sci. U. S. A.* **2018**, *115*, 9026−9031.

(10) Hanemann, T.; Szabo, D. V. Polymer-Nanoparticle Composites: From Synthesis to Modern Applications. *Materials* **2010**, *3*, 3468−3517.

(11) Yan, L. T.; Xie, X. M. Computational Modeling and Simulation of Nanoparticle Self-Assembly in Polymeric Systems: Structures, Properties and External Field Effects. *Prog. Polym. Sci.* **2013**, *38*, 369−405.

(12) Mangal, R.; Srivastava, S.; Archer, L. A. Phase Stability and Dynamics of Entangled Polymer-Nanoparticle Composites. *Nat. Commun.* **2015**, *6*, 7198.

(13) Quaresimin, M.; Schulte, K.; Zappalorto, M.; Chandrasekaran, S. Toughening Mechanisms in Polymer Nanocomposites: From Experiments to Modelling. *Compos. Sci. Technol.* **2016**, *123*, 187−204.

(14) Kumar, S. K.; Ganesan, V.; Riggleman, R. A. Perspective: Outstanding Theoretical Questions in Polymer-Nanoparticle Hybrids. *J. Chem. Phys.* **2017**, *147*, 020901.

(15) Kumar, S. K.; Benicewicz, B. C.; Vaia, R. A.; Winey, K. I. 50th Anniversary Perspective: Are Polymer Nanocomposites Practical for Application ? *Macromolecules* **2017**, *50*, 714−730.

(16) Dai, X.; Hou, C.; Xu, Z.; Yang, Y.; Zhu, G.; Chen, P.; Huang, Z.; Yan, L. Entropic Effects in Polymer Nanocomposites. *Entropy* **2019**, *21*, 186.

(17) Roth, R.; Evans, R.; Dietrich, S. Depletion Potential in Hard-Sphere Mixtures: Theory and Applications. *Phys. Rev. E: Stat. Phys., Plasmas, Fluids, Relat. Interdiscip. Top.* **2000**, *62*, 5360−5377.

(18) Cao, X. Z.; Merlitz, H.; Wu, C. X.; Sommer, J. U. Polymer-Induced Entropic Depletion Potential. *Phys. Rev. E* **2011**, *84*, 041802.

(19) Zhu, G. L.; Huang, Z. H.; Xu, Z. Y.; Yan, L. T. Tailoring Interfacial Nanoparticle Organization through Entropy. *Acc. Chem. Res.* **2018**, *51*, 900−909.

(20) Cao, X. Z.; Merlitz, H.; Wu, C. X.; Egorov, S. A.; Sommer, J. U. Effective Pair Potentials between Nanoparticles Induced by Single Monomers and Polymer Chains. *Soft Matter* **2013**, *9*, 5916−5926.

(21) Semenov, A. N.; Shvets, A. A. Theory of Colloid Depletion Stabilization by Unattached and Adsorbed Polymers. *Soft Matter* **2015**, *11*, 8863−8878.

(22) Feng, L.; Laderman, B.; Sacanna, S.; Chaikin, P. Re-Entrant Solidification in Polymer-Colloid Mixtures as A Consequence of Competing Entropic and Enthalpic Attractions. *Nat. Mater.* **2015**, *14*, 61−65.

(23) Xie, F.; Woodward, C. E.; Forsman, J. Non-Monotonic Temperature Response of Polymer Mediated Interactions. *Soft Matter* **2016**, *12*, 658−663.

(24) Cao, X. Z.; Merlitz, H.; Wu, C. X.; Ungar, G.; Sommer, J. U. A Theoretical Study of Dispersion-to-Aggregation of Nanoparticles in Adsorbing Polymers Using Molecular Dynamics Simulations. *Nanoscale* **2016**, *8*, 6964−6968.

(25) Glomann, T.; Schneider, G. J.; Allgaier, J.; Radulescu, A.; Lohstroh, W.; Farago, B.; Richter, D. Microscopic Dynamics of Polyethylene Glycol Chains Interacting with Silica Nanoparticles. *Phys. Rev. Lett.* **2013**, *110*, 178001.

(26) Krutyeva, M.; et al. Effect of Nanoconfinement on Polymer Dynamics: Surface Layers and Interphases. *Phys. Rev. Lett.* **2013**, *110*, 108303.

(27) Holt, A.; Griffin, P.; Bocharova, V.; Agapov, A.; Imel, A.; Dadmun, M.; Sangoro, J.; Sokolov, A. Dynamics at The Polymer/Nanoparticle Interface in Poly(2-vinylpyridine)/Silica Nanocomposites. *Macromolecules* **2014**, *47*, 1837−1843.

(28) Senses, E.; Narayanan, S.; Mao, Y.; Faraone, A. Nanoscale Particle Motion in Attractive Polymer Nanocomposites. *Phys. Rev. Lett.* **2017**, *119*, 237801.

(29) Kremer, K.; Grest, G. S. Dynamics of Entangled Linear Polymer Melts: A Molecular-Dynamics Simulation. *J. Chem. Phys.* **1990**, *92*, 5057−5086.

(30) Plimpton, S. Newblock Fast Parallel Algorithms for Short-Range Molecular Dynamics. *J. Comput. Phys.* **1995**, *117*, 1.

(31) Dünweg, B.; Paul, W. Newblock Brownian Dynamics Simulations without Gaussian Random Numbers. *Int. J. Mod. Phys. C* **1991**, *02*, 817.

DOI: 10.1021/acs.jpclett.9b01954
J. Phys. Chem. Lett. 2019, 10, 4968−4973

(32) Iwaoka, N.; Hagita, K.; Takano, H. Estimation of Relaxation Modulus of Polymer Melts by Molecular Dynamics Simulations: Application of Relaxation Mode Analysis. *J. Phys. Soc. Jpn.* **2015**, *84*, 044801.
(33) Lee, W. B.; Kremer, K. Entangled Polymer Melts: Relation between Plateau Modulus and Stress Autocorrelaton Function. *Macromolecules* **2009**, *42*, 6270−6276.
(34) Likhtman, A. E.; Sukumaran, S. K.; Ramirez, J. Linear Viscoelasticity from Molecular Dynamics Simulation of Entangled Polymers. *Macromolecules* **2007**, *40*, 6748−6757.
(35) McLeish, T. C. B. Tube Theory of Entangled Polymer Dynamics. *Adv. Phys.* **2002**, *51*, 1379−1527.
(36) Smith, G. D.; Bedrov, D.; Li, L. W.; Byutner, O. A Molecular Dynamics Simulation Study of The Viscoelastic Properties of Polymer Nanocomposites. *J. Chem. Phys.* **2002**, *117*, 9478.
(37) Pryamitsyn, V.; Ganesan, V. Origins of Linear Viscoelastic Behavior of Polymer-Nanoparticle Composites. *Macromolecules* **2006**, *39*, 844−856.
(38) Senses, E.; Faraone, A.; Akcora, P. Microscopic Chain Motion in Polymer Nanocomposites with Dynamically Asymmetric Interphases. *Sci. Rep.* **2016**, *6*, 29326.
(39) Kopf, A.; Dünweg, B.; Paul, W. Dynamics of Polymer "Isotope" Mixtures: Molecular Dynamics Simulation and Rouse Model Analysis. *J. Chem. Phys.* **1997**, *107*, 6945.
(40) Rauscher, P. M.; Rowan, S. J.; de Pablo, J. J. Topological Effects in Isolated Poly[n]catenanes: Molecular Dynamics Simulations and Rouse Mode Analysis. *ACS Macro Lett.* **2018**, *7*, 938−943.
(41) Cao, X. Z.; Merlitz, H.; Wu, C. X. Tuning Adsorption Duration To Control the Diffusion of a Nanoparticle in Adsorbing Polymers. *J. Phys. Chem. Lett.* **2017**, *8*, 2629−2633.
(42) Hooper, J. B.; Schweizer, K. S. Contact Aggregation, Bridging, and Steric Stabilization in Dense Polymer-Particle Mixtures. *Macromolecules* **2005**, *38*, 8858−8869.
(43) Senses, E.; et al. Small Particle Driven Chain Disentanglements in Polymer Nanocomposites. *Phys. Rev. Lett.* **2017**, *118*, 147801.

DOI: 10.1021/acs.jpclett.9b01954
J. Phys. Chem. Lett. 2019, 10, 4968−4973